Crystal Structure Reveals the Binding Mode and Selectivity of a Photoswitchable Ligand for the Adenosine A_{2A} Receptor

Tsuyoshi Araya,[a‡] Yuya Matsuba,[b‡] Harufumi Suzuki,[b‡] Tomohiro Doura,[b‡] Nipawan Nuemket,[c,d] Eriko Nango,[c,e] Masaki Yamamoto,[c] Dohyun Im,[a] Hidetsugu Asada,*[a] Shigeki Kiyonaka,*[b,f] and So Iwata*[a,c]

[a]Department of Cell Biology, Graduate School of Medicine, Kyoto University, Kyoto 606-8501, Japan.
[b]Department of Biomolecular Engineering, Graduate School of Engineering, Nagoya University, Nagoya 464-8603, Japan
[c]RIKEN SPring-8 Center, Hyogo 679-5148, Japan
[d]JASRI, Hyogo 679-5148, Japan
[e]Institute of Multidisciplinary Research for Advanced Materials, Tohoku University, Miyagi 980-8577, Japan
[f]Institute of Nano-Life-Systems, Institutes of Innovation for Future Society, Nagoya University, Nagoya 464-8603, Japan

*Correspondence: asada.hidetsugu.4s@kyoto-u.ac.jp
kiyonaka@chembio.nagoya-u.ac.jp
iwata.so.2z@kyoto-u.ac.jp

‡These authors contributed equally to this work.

Abstract

Rational synthetic expansion of photoresponsive ligands is important for photopharmacological studies. In this study, the photoresponsive and receptor-selective ligand, photoNECA(blue), was synthesized for the adenosine A_{2A} receptor, and its crystal structure was determined. This complex structure explains the binding mode and photoresponsive mechanism of photoNECA(blue).

Main text

In photopharmacology, photoresponsive compounds spatiotemporally regulate the function of target molecules.[1] Photoswitchable ligands, which are photoresponsive compounds, generate geometric isomers depending on the wavelength of irradiation, and the isomers show different affinities, functions, and signaling activities for their targets. Several photoswitchable ligands have been developed for various target proteins.[2]

One important target for photopharmacology is G protein-coupled receptors (GPCRs).[3] GPCRs play an important role in several physiological processes, including the maintenance of homeostasis, and are important drug targets for numerous human diseases.[4] The adenosine receptors among GPCRs have four subtypes (A_1R, $A_{2A}R$, $A_{2B}R$, and A_3R). $A_{2A}R$ plays an important role in the regulation of glutamate and dopamine release in the brain. In other tissues, it plays various roles such as increasing coronary circulation by regulating myocardial oxygen demand and protecting tissues from inflammation by suppressing immune cells. As such, it is considered a therapeutic target for various diseases, including Parkinson's disease and cancer.[5,6] Therefore, the spatiotemporal regulation of $A_{2A}R$ function may lead to an understanding of $A_{2A}R$-associated diseases and the development of treatment modalities.

Structure-based drug design is useful in the rational design of ligands.[7] In particular, structural information on the compound-bound target molecules can successfully explain the pharmacological findings of the compounds and thus plays a significant role in improving the selectivity and function of the compounds. $A_{2A}R$ is known as one of the most crystalline GPCRs, and various crystal structures of its active conformations have been obtained.[8-13] Notably, potential photoswitchable ligands have been reported for $A_{2A}R$.[14-16] Therefore, we performed X-ray crystal structure analyses of photoswitchable ligand-bound $A_{2A}R$ complexes for the rational design of structure-based photoswitchable ligands and to elucidate the photoswitching mechanism.

Initial studies on the crystallization of $A_{2A}R$ with a photoswitchable ligand were performed using MRS5543[14] or photoAd(blue)[15] as the ligands. Although complex crystals were obtained, their structures could not be determined because of their low resolution (data not shown). This may be because the receptor-stabilizing effect of the ligands has not yet reached the level of structural determination. Thus, we designed a new photoswitchable ligand **1** for $A_{2A}R$ for crystal structure analysis, focusing on photoAd(blue), which has a higher affinity than MRS5543 (Fig. S1a, Scheme S1). **1** contains 5'-*N*-ethylcarboxamidoadenosine (NECA) instead of adenosine as the ligand group. NECA is a non-selective but high-affinity agonist for the adenosine receptors, in which the C5' of the ribose ring is replaced with an *N*-ethylcarboxyamide group. Because NECA is the most widely used ligand in crystal structure

analyses of agonist-bound $A_{2A}R$,[9,11] it was considered a suitable agonist moiety for this study. The photoisomerization ability of **1** was evaluated using ultraviolet–visible (UV-vis) absorption spectrometry. As shown in Fig. 1b, irradiation of 365 nm LED caused the decrease in absorbance around 312 nm corresponding to the π–π* transition absorption band of the *trans*-isomer. This indicates *trans*-to-*cis* photoisomerization of **1**. The isomeric ratio determined by ^{1}H NMR spectroscopy showed that 75% of the *trans*-isomer was photoconverted to the *cis*-isomer after 365 nm irradiation (Fig. S1b), and the *cis*-isomer was relatively stable [half-life ($t_{1/2}$) = 32 h] at 37 ℃ (Fig. S1c). In adenosine receptor-expressing HEK293 cells, half-maximal effective concentration (EC_{50}) values for $A_{2A}R$ activation were calculated for the *trans*- and *cis*-isomers of **1**. As shown in Fig. 1c, the EC_{50} value of the *trans*-isomer was 27 ± 2.4 nM, while that of the *cis*-isomer was >1000 nM. In addition, the EC_{50} value of the *trans*-isomer of **1** for A_1R was >1000 nM, showing high subtype selectivity for the compound among the adenosine receptor family (Fig. S1d). These results indicated that **1** acts as a potential photoswitchable ligand for crystal structure studies, and we named **1** photoNECA(blue).

We also designed a new thermostabilized mutant $A_{2A}R$-Rag31 for crystal structure analyses. $A_{2A}R$-Rag31 was expressed in *Spodoptera frugiperda* (Sf9) insect cells, and its purification and crystallization were performed in the presence of *trans*-photoNECA(blue) under dark and/or red light (640–660 nm) to prevent light-induced *trans*-to-*cis* isomerization (Fig. S2a). The purified *trans*-photoNECA(blue)-bound receptor was complexed with the specific structure-recognition antibody fragment Fab94-1 (Im *et al*., manuscript in preparation) for agonist-bound $A_{2A}R$ as a crystallization facilitating binder. This complex was obtained by gel filtration (Fig. S2b and S2c). The complex was crystallized using the lipid cubic phase crystallization method (Fig. S2d). Subsequently, 391 datasets were collected at SPring-8 beamline BL32XU, and the structure was determined at 3.34-Å resolution via phase determination by molecular replacement method and refinement using Phenix software (Fig. 2a, Table S1). The electron density map identified in the ligand-binding pocket allowed us to determine the structure of *trans*-photoNECA(blue) (Fig. 2b). In contrast, the N-terminal region (residues 1–2), extracellular loop 2 (ECL2) region (residues 148–155), and C-terminal region (residues 308–316) of $A_{2A}R$-Rag31 had insufficient electron density for model construction. When we compared our structure with the NECA-bound $A_{2A}R$-GL31 structure [Protein Data Bank identification number (PDB ID):2YDV], the root mean square deviation (RMSD) of all residues was almost identical at 0.563 Å, suggesting that our structure is similar to the NECA-bound $A_{2A}R$-GL31 structure. These results demonstrated the reliability of the proposed structure.

The binding mode of the NECA moiety of *trans*-photoNECA(blue) in the receptor was similar to that of the NECA-bound receptor structure (PDB ID:2YDV) with a RMSD of 0.305 Å (Fig. 2c). In particular, the hydrogen bonds formed between the NECA and the six residues of the receptor (Thr88$^{3.36}$, His250$^{6.52}$, Asn253$^{6.55}$, Ser277$^{7.42}$, Glu169^{ECL2}, and His278$^{7.43}$) (Superscripts are based on Ballesteros–Weinstein numbering stored in GPCRs.[17]), as well as the π-stacking interactions between the adenine moiety of the NECA and Phe168^{ECL2} of the receptor, were also conserved in *trans*-photoNECA(blue) (Fig. 2c). The identity of these interactions observed in both *trans*-photoNECA(blue) and NECA structures explains the high signaling activity of *trans*-photoNECA(blue) for $A_{2A}R$. In contrast, the azobenzene moiety of *trans*-photoNECA(blue) was oriented extracellularly away from the NECA-binding moiety (Fig. 2c). The azobenzene moiety was accommodated in a hydrophobic pocket consisting of four residues of the receptor (Ser67$^{2.65}$, Leu167^{ECL2}, Leu267$^{7.32}$, and Tyr271$^{7.36}$) (Fig. 3a and 3b). Although this hydrophobic pocket was not utilized in the interaction with NECA, the side-chain orientations were consistent with the structures revealed in this study. Therefore, it is evident that *trans*-photoNECA(blue) successfully utilizes this hydrophobic pocket, which is a common motif independent of the ligand.

Trans-photoNECA(blue) has high signaling activity for $A_{2A}R$, whereas the *cis*-isomer has lower signaling activity. To understand this, a model structure, in which the *trans*-photoNECA(blue) structure was replaced by the *cis*-photoNECA(blue) structure, was developed (Fig. 3c). These results suggested that in the *cis*-photoNECA(blue)-bound model structure, the photoswitching moiety of the ligand, was completely removed from the hydrophobic pocket. This can be a destabilizing factor for the ligand. Furthermore, the benzene ring of the photoswitching moiety of *cis*-photoNECA(blue) may cause steric hindrance in the ligand-binding pocket, where the polar amino acid is localized (Fig. S3). The photoswitching moiety of photoNECA(blue) is hydrophobic and therefore repulsive to polar residues, which may be a factor in the dissociation of the *cis*-isomer from the receptor. These possibilities, revealed by the model structure, may explain the loss of the *cis*-isomer signaling activity of the *cis*-isomer.

PhotoAd (blue), based on photoNECA(blue), is also an $A_{2A}R$-selective photoswitchable ligand with low affinity for the A_1R subtype.[15] In contrast, adenosine and NECA have no subtype selectivity for adenosine receptors. This indicates that the photoswitching moiety of photoNECA(blue) is important for $A_{2A}R$ selectivity. The receptor selectivity of photoNECA(blue) is discussed based on our structure. In $A_{2A}R$, the hydrophobic pocket containing Ser67$^{2.65}$, Leu167^{ECL2}, Leu267$^{7.32}$, and Tyr271$^{7.36}$ was composed of polar residues (N70$^{2.65}$, E170^{ELC2}, S267$^{7.32}$, and Y271$^{7.36}$) in the NECA-bound A_1R structure (PDB ID:6D9H),

suggesting that the photoswitching moiety may repel the polar pocket in A_1R (Fig. S4). The differences in these pockets may contribute to the receptor selectivity of photoswitchable ligands. This indicates that the photoswitching moiety of photoAd(blue) and photoNECA(blue) plays an important role in not only the photoswitching mechanism, but also receptor subtype selectivity. In structural studies of the complex with the $A_{2A}R$-selective antagonist Cmpd-1, an allosteric pocket that contributes to selectivity for $A_{2A}R$ has been reported,[18] and as our hydrophobic pocket confers similar selectivity (Fig. S5), it is interesting to note that these allosteric regions are available for selectivity.

In conclusion, we developed a novel photoswitchable ligand, photoNECA(blue), for $A_{2A}R$, and successfully determined the X-ray crystal structure of its complex by conformational stabilization of $A_{2A}R$. From three-dimensional structural analysis, it was possible to discuss the mechanism of photoswitching and its selectivity for $A_{2A}R$ (Fig. 4). These results are expected to facilitate the rational design of $A_{2A}R$ photoswitchable ligands in the near future. Recently, time-resolved structural studies using X-ray free-electron lasers have attracted considerable attention for elucidating the activation mechanism of GPCRs at atomic resolution.[19] This technique has revealed the detailed activation mechanism of bovine rhodopsin. However, structural analyses are limited to light-driven GPCRs. In this study, we successfully demonstrated light-driven activation of $A_{2A}R$ and determined its X-ray crystal structure. Therefore, this study is expected to strongly promote not only the rational design of photoresponsive ligands but also dynamic structural studies of $A_{2A}R$.

Crystal structure information was deposited in the Protein Data Bank (accession number 8WDT).

Conflicts of interest

The authors declare no competing financial interests.

Notes and references

1. W. A. Velema, W. Szymanski and B. L. Feringa, *J. Am. Chem. Soc.*, 2014, **136**, 2178–2191.
2. P. Kobauri, F. J. Dekker, W. Szymanski and B. L. Feringa, *Angew. Chemie - Int. Ed.*, 2023, **62**, 1–62.
3. M. Ricart-ortega, J. Font and A. Llebaria, *Mol. Cell. Endocrinol.*, 2019, **488**, 36–51.
4. S. Hauser, M. M. Attwood, M. Rask-Andersen, H. B. Schiöth and D. E. Gloriam, *Nat. Rev. Drug Discov.*, 2017, **16**, 829–842.
5. R. Franco and G. Navarro, *Front. Psychiatry*, 2018, **9**, 1–5.
6. C. Sun, B Wang and S. Hao, *Front. Immunol.*, 2022, **13**, 1-9
7. L. G. Ferreira, R. N. Dos Santos, G. Oliva and A. D. Andricopulo, *molecules*, 2015, **20**, 13384–13421.
8. F. Xu, H. Wu, V. Katritch, G. W. Han, K. A. Jacobson, Z.-G. Gao, V. Cherezov and R. C. Stevens, *Science.*, 2011, **332**, 322–327.
9. G. Lebon, T. Warne, P. C. Edwards, K. Bennett, C. J. Langmead, A. G. W. Leslie and C. G. Tate, *Nature*, 2011, **474**, 521–526.
10. G. Lebon, P. C. Edwards, A. G. W. Leslie and C. G. Tate, *Mol. Pharmacol.*, 2015, **87**, 907–915.
11. B. Carpenter, R. Nehmé, T. Warne, A. G. W. Leslie and C. G. Tate, *Nature*, 2016, **536**, 104–107.
12. T. Amelia, J. P. D. Van Veldhoven, M. Falsini, R. Liu, L. H. Heitman, G. J. P. Van Westen, E. Segala, G. Verdon, R. K. Y. Cheng, R. M. Cooke, D. Van Der Es and A. P. Ijzerman, *J. Med. Chem.*, 2021, **64**, 3827–3842.
13. M. Cui, Q. Zhou, Y. Xu, Y. Weng, D. Yao, S. Zhao and G. Song, *IUCrJ*, 2022, **9**, 333–341.
14. M. I. Bahamonde, J. Taura, S. Paoletta, A. A. Gakh, S. Chakraborty, J. Hernando, V. Fernández-Dueñas, K. A. Jacobson, P. Gorostiza and F. Ciruela, *Bioconjug. Chem.*, 2014, **25**, 1847–1854.
15. H. Suzuki, T. Doura, Y. Matsuba, T. Araya, H. Asada, S. Iwata and S. Kiyonaka, Manuscript in preparation.
16. K. Hüll, V. Fernández-Dueñas, M. Schönberger, M. lópez-Cano, D. Trauner and F. Ciruela, *Bioconjugate Chem*. 2021, **32**, 1979–1983.
17. J. A. Ballesteros and H. Weinstein, *Methods Neurosci.* 1995, **25**, 366-428.

18. B. Sun, P. Bachhawat, M. L. H. Chu, M. Wood, T. Ceska, Z. A. Sands, J. Mercier, F. Lebon, T. S. Kobilka and B. K. Kobilka, *Proc. Natl. Acad. Sci. U. S. A.*, 2017, **114**, 2066–2071.
19. T. Gruhl, T. Weinert, M. J. Rodrigues, C. J. Milne, G. Ortolani, K. Nass, E. Nango, S. Sen, P. J. M. Johnson, C. Cirelli, A. Furrer, S. Mous, P. Skopintsev, D. James, F. Dworkowski, P. Båth, D. Kekilli, D. Ozerov, R. Tanaka, H. Glover, C. Bacellar, S. Brünle, C. M. Casadei, A. D. Diethelm, D. Gashi, G. Gotthard, R. Guixà-González, Y. Joti, V. Kabanova, G. Knopp, E. Lesca, P. Ma, I. Martiel, J. Mühle, S. Owada, F. Pamula, D. Sarabi, O. Tejero, C. J. Tsai, N. Varma, A. Wach, S. Boutet, K. Tono, P. Nogly, X. Deupi, S. Iwata, R. Neutze, J. Standfuss, G. Schertler and V. Panneels, *Nature*, 2023, **615**, 939–944.

ORCID

Tsuyoshi Araya: 0000-0002-7197-1053

Tomohiro Doura: 0000-0003-1826-6010

Eriko Nango: 0000-0001-9851-7355

Masaki Yamamoto: 0000-0002-1311-1768

Dohyun Im: 0000-0002-6939-7718

Hidetsugu Asada: 0000-0001-6255-4728

Shigeki Kiyonaka: 0000-0002-4100-6738

So Iwata: 0000-0003-1735-2937

ACKNOWLEDGEMENTS

This work was supported by JSPS Grant-in-Aid for Scientific Research on Innovative Areas (Grant Number 19H05777 to S.I., 19H05778 to S.K., 19H05781 to E.N.), Research Support Project for Life Science and Drug Discovery (BINDS) from AMED (Grant Number JP23ama121001 to M.Y., JP23ama121007 to S.I.), Platform Project for Supporting Drug Discovery and Life Science Research (BINDS) from AMED (Grant Number JP21am0101070 to M.Y., JP21am0101079 to S.I.), Fostering Joint International Research (B) (Grant Number 22KK0099 to H.A.), JST ERATO Hamachi Innovative Molecular Technology for Neuroscience Project (Grant Number JPMJER1802 to S.K.), and Kyoto University MIP Interdisciplinary Joint Research grant to T.A.. We thank K. Hirata, Y. Kawano, and H. Matsuura at BL32XU of SPring-8 for their technical assistance, T. Murata, S. Ogasawara and T. Hino for obtaining Fab94-1, and H. Ago and C. Higuchi for their technical assistance in the dark and/or red light room experiments.

FIGURES

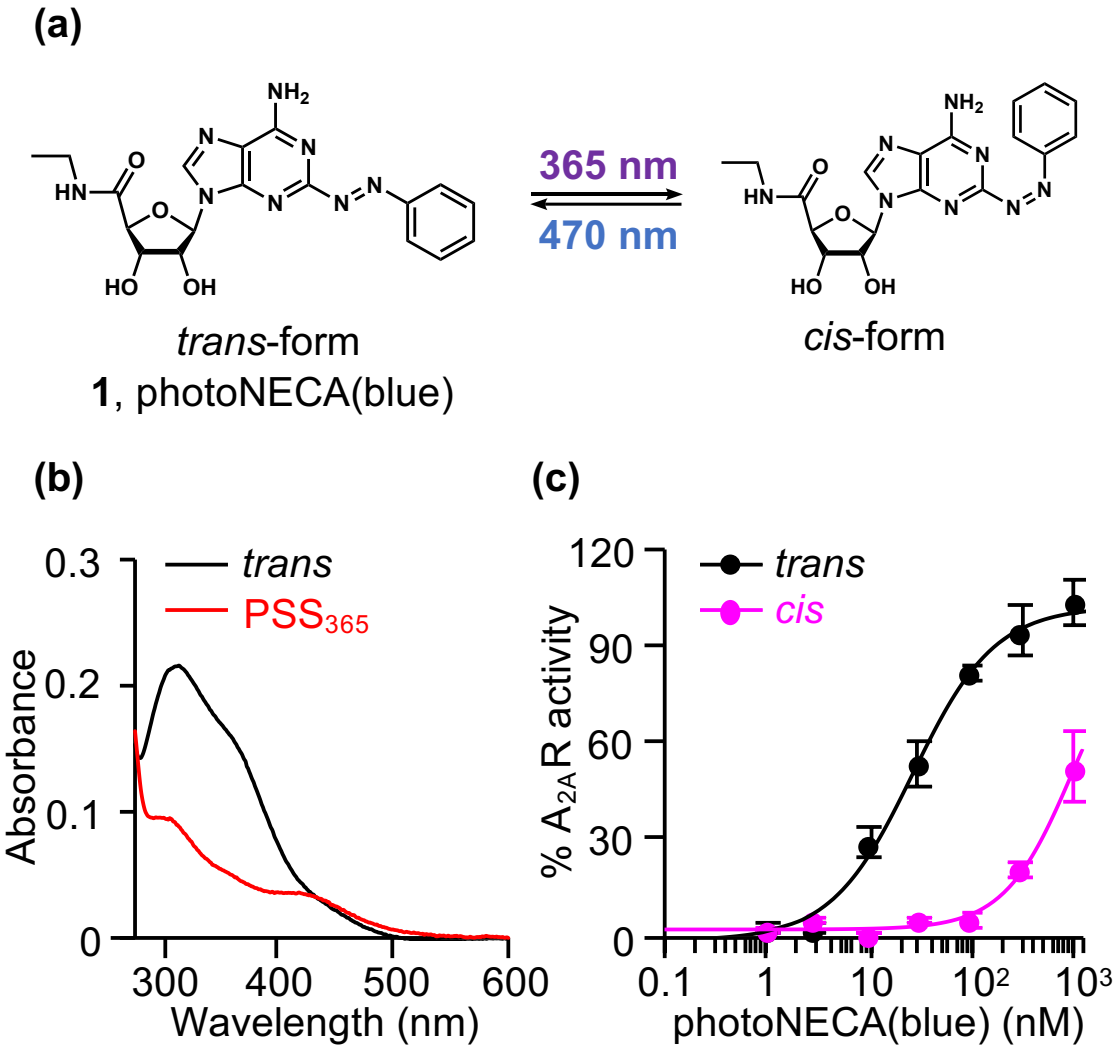

Fig 1. Photochemical and pharmacological properties of photoNECA(blue). (a) A schematic of the photoisomerization of photoNECA(blue) by 365 nm or 470 nm light. (b) The UV−vis absorption spectra of *trans*-photoNECA(blue) (black) and the 365 nm-adapted photostationary state (PSS_{365}, red). (c) Activity of *trans*- (black) and *cis*-photoNECA(blue) (magenta) for $A_{2A}R$. Percentage of $A_{2A}R$ activity was determined using the value activated by 1 μM adenosine as 100% (N = 3). Error bars indicate the standard error of the mean (SEM).

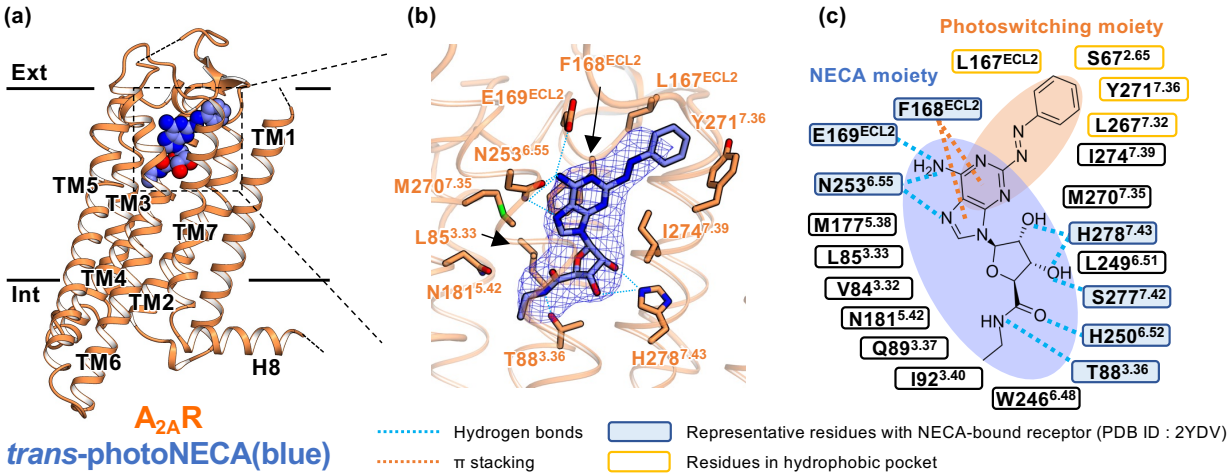

Fig 2. Structure of *trans*-photoNECA(blue)-bound A_{2A}R-Rag31. (a) Side view of the *trans*-photoNECA(blue)-bound A_{2A}R-Rag31 structure. The receptor and ligand are shown as a ribbon model in orange and a CPK space-filling model in blue, respectively. (b) Close-up view of the ligand-binding pocket of *trans*-photoNECA(blue)-bound A_{2A}R-Rag31. The omitted mF_o–DF_c electron density (blue mesh) contoured at 3.0 σ. The ligand and representative residues within 4.0 Å distance of the ligand are shown as stick models in blue and orange, respectively. The receptor is shown as a ribbon model. Hydrogen bonds in the receptor are shown as skyblue dashed lines. (c) Diagram of the interactions between *trans*-photoNECA(blue) and A_{2A}R-Rag31. All residues within 4.0 Å distance of the ligands are shown. The NECA moiety and photoswitching moiety of the ligand are shown in the closed blue and orange circles, respectively.

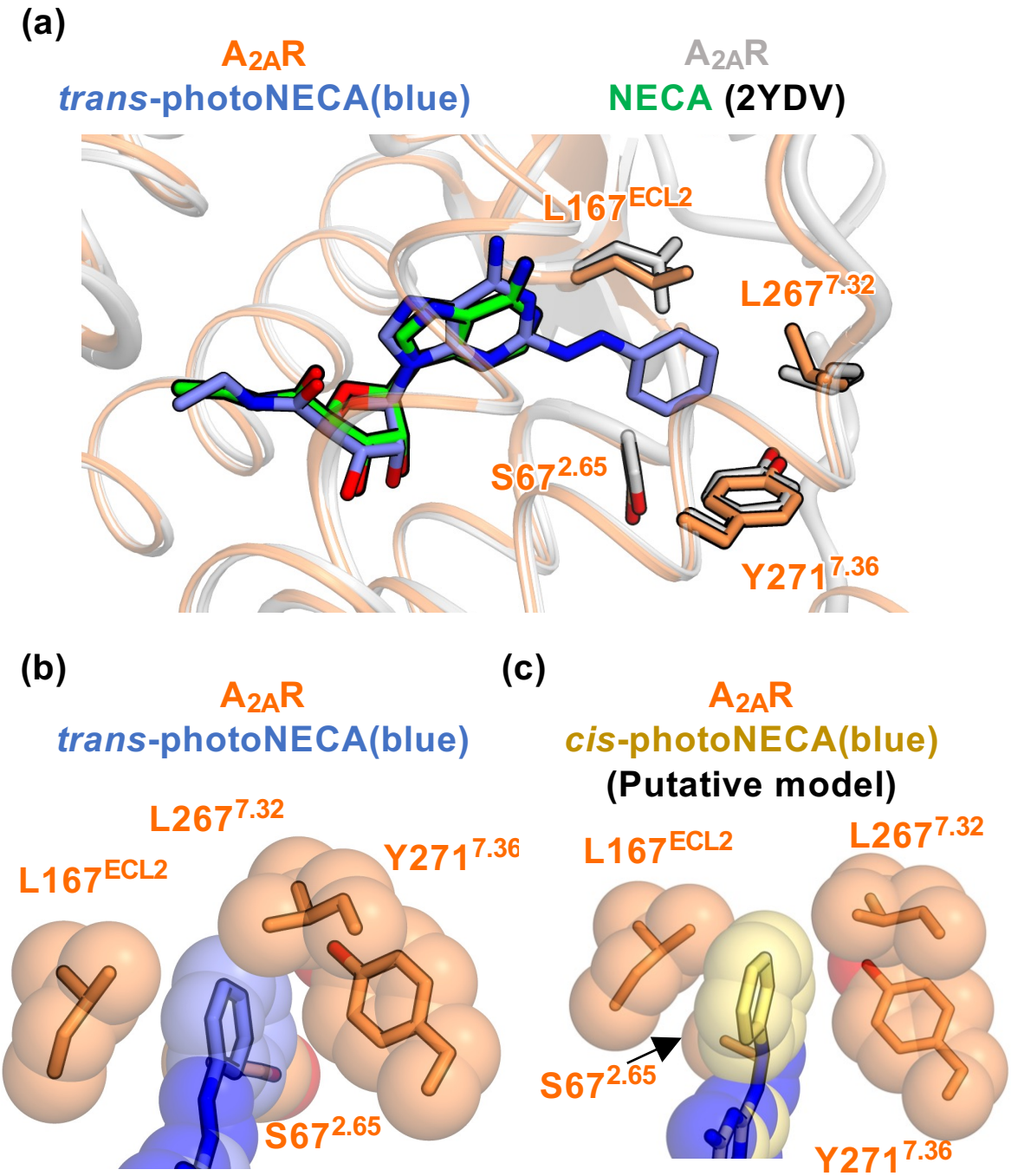

Fig 3. Interactions of photoswitching moiety of *trans*- and *cis*-photoNECA(blue). (a) The structural comparison of *trans*-photoNECA(blue)-bound and NECA-bound $A_{2A}R$ (PDB ID : 2YDV). Ligands and representative residues are shown as stick models. Receptors are shown as ribbon models. (b,c) The interactions between the photoswitching moiety of *trans*-photoNECA(blue) in (b) and *cis*-photoNECA(blue) in (c). Residues of the hydrophobic pocket of $A_{2A}R$-Rag31 are highlighted, and ligands and residues are shown as CPK space-filling models. $A_{2A}R$-Rag31 and $A_{2A}R$-GL31 are indicated in orange or gray, respectively. *Trans*-, *cis*-photoNECA(blue), and NECA are indicated in blue, yellow, and green, respectively.

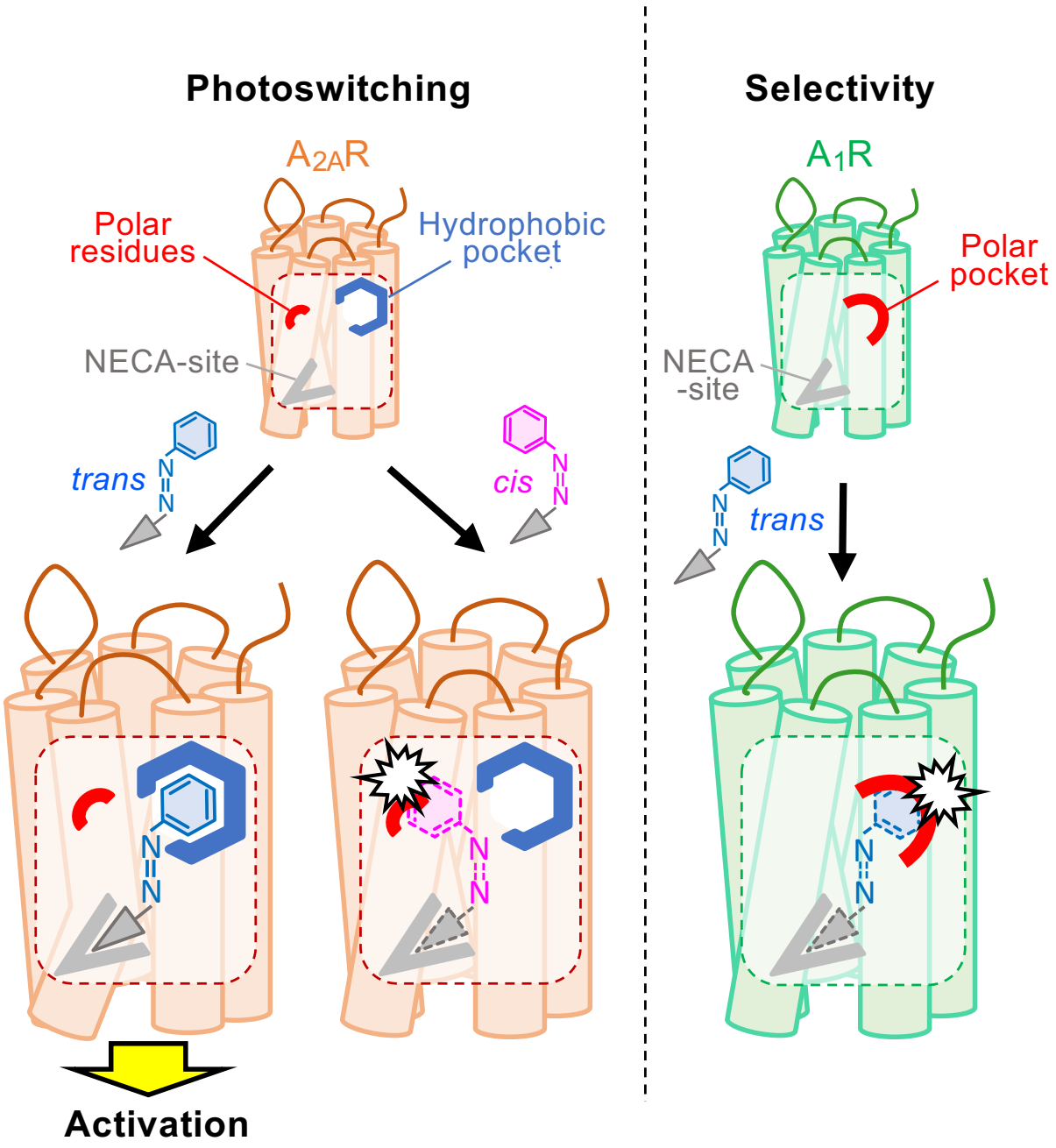

Fig 4. Schematic illustration of the photoswitching and selective action of photoNECA(blue) for $A_{2A}R$.